

Occluding Junctions of the *Necturus* Gallbladder

M. Cerejido, E. Stefani, and B. Chávez de Ramírez

Centro de Investigación y Estudios Avanzados del I.P.N., Departamentos de Fisiología y Biofísica y de Biología Celular, Apartado Postal 14-740 México, D.F. 07000, Mexico

Summary. The paracellular conducting pathway of the *Necturus* gallbladder was studied with electrophysiological and electromicroscopic methods. The first one consists of the passage of short (5 msec) and small ($32 \mu\text{A cm}^{-2}$) current pulses associated with a voltage scanning of the plane of the epithelium at the apical surface with a microelectrode to detect the regions where current flows. The procedure shows that (a) the conductance is evenly distributed along the intercellular regions along the intercellular spaces of the cells where occluding junctions are located; (b) the field above the occluding junctions has the shape of a bell, so that the junction can be sensed at 1–2 μm from the region where the intercellular space is visualized by light microscopy; (c) the intersections between three cells, in spite of having 3 half-junctions contributing (instead of two), do not have a higher conductance than the rest of the occluding junction. Scanning electron microscopy shows that (a) cells are densely covered by microvilli which interdigitate above the region of the occluding junctions, and (b) are covered by a surface coat. With transmission electron microscopy, (a) the opening of the occluding junctions at the apical border appears irregular, and most of them oblique; (b) in the last microns the actual mouth of the junction may deviate from the course of the interspace. Freeze-fracture replicas indicate that (a) the occluding junction has a uniform width and little variations in the number of strands around the cell, except (b) at intersections between 3 cells where both, its width and the number of strands, increase toward the basal region.

Key Words paracellular route · occluding junctions · voltage scanning · epithelial membranes · gallbladder

Introduction

The location of the pathway of high electrical conductance in the *Necturus* gallbladder was studied using a method analogous to the one developed by Frömter (1972) and Frömter and Diamond (1972). Both methods are based on the passage of an electric current through the epithelium, and the scanning of the apical surface with a microelectrode to detect the points where current flows. Our method was originally developed to study cultured monolayers of MDCK cells (an epithelioid line of

renal origin) (Cerejido, Stefani & Martínez-Palomo, 1980). These monolayers can be cultured on permeable supports and mounted between two chambers where they exhibit the properties of natural epithelia (Misfeldt, Hamamoto & Pitelka, 1976; Cerejido, Robbins, Dolan, Rotunno & Sabatini, 1978). Yet since they are not natural epithelia, we had to demonstrate that the low resistance of the monolayers ($80\text{--}150 \Omega \text{cm}^2$) was actually due to a paracellular permeation route, rather than to incomplete growth or faulty sealing. Once the study was performed in the cultured epithelial cells, we wanted to apply the procedure to a natural transporting epithelium for comparison, and we turned to the *Necturus* gallbladder where the data obtained by Frömter and Diamond were available. However, Bindslev, Tormey and Wright (1974) have studied the changes in ion conductivities induced by electric currents in tight as well as leaky epithelia, and have shown that the high direct currents, of the kind used in the *Necturus* gallbladder, not only influence properties of cellular interspaces, but also of cell membranes. Furthermore, Reuss and Finn (1977), have reported that current clamps bring about significant changes on trans-epithelial and cell membrane resistance in *Necturus* gallbladder, suggesting the accumulation or depletion of intracellular potassium (see Reuss, 1978). As discussed below, these objections may not apply to the method that we devised and that is used in this article.

Our previous study of MDCK monolayers (Cerejido et al., 1980) indicated that, although the shunt pathway is located at the intercellular space, conductance is not evenly distributed along this space, but is best represented by an actually tight junction studded with conducting spots. Since in that study we also analyzed the distribution of the strands of the occluding junctions in freeze-fraction

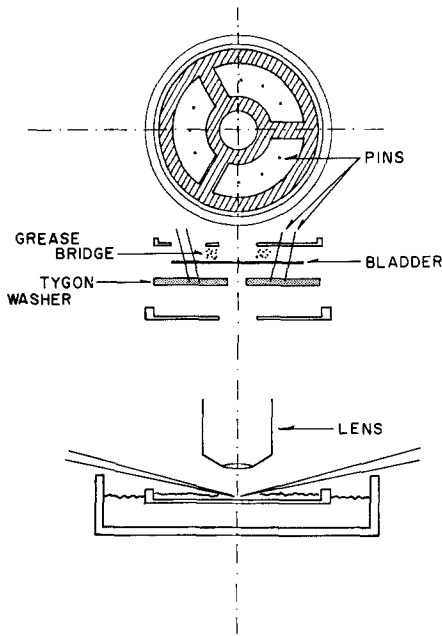


Fig. 1. Middle. Exploded view of the Lucite® chamber used to map the surface of the *Necturus* gallbladder. The tissue is pinned with the apical side up to a Tygon washer. Stretching is very mild, just enough to obtain some planar regions. The upper part of the chamber (represented above) consists of a central ring intended to press the tissue, an open area that leaves way for the pins, and a peripheral portion. The grease bridge is composed of 10% Vaseline® and 90% paraffin which makes the mixture harder and stable. Below: The whole assembly is placed on a 10-cm petri dish. A 40× water immersion lens controls the positioning of two microelectrodes (one explorer, another reference) maneuvered with two Huxley micromanipulators. Current is delivered via two rings of chlorided silver (not shown)

ture replicas, and observed that their number varies abruptly from 1 to 10 within a few nanometers, the possibility arose that the points of high and low conductance would correspond to regions with few or many strands, respectively. Therefore, we wanted to study a natural epithelium like the *Necturus* gallbladder that, as shown below, has structurally uniform occluding junctions.

Materials and Methods

Electrophysiological Methods

Necturi were obtained from Lemberger Co. (Oshkosh, Wisconsin). Animals were kept at room temperature (20–22 °C) in plastic water tanks gassed with compressed air. The gallbladder was dissected, taking care to avoid contact of the bile with the serosa, and mounted between two conventional Lucite® chambers to study electrical properties.

Total Membrane Resistance and Capacity. Gallbladders were mounted as a diaphragm between two Lucite® chambers of 2.5 ml each. The exposed area was 0.2 cm². Current was delivered from a square pulse generator whose output was connected

to a chlorided silver electrode via a 10 KΩ resistor. It was collected through a second electrode placed on the opposite chamber, which was virtually grounded via a current-voltage converter with a 10 KΩ resistor in the negative feedback loop. The current pulse was displayed in a cathode ray oscilloscope (CRO). The voltage deflection across the preparation produced by the current flow was measured with two chlorided silver electrodes placed at less than 1 mm from each side of the tissue. They were connected to high input impedance amplifiers (voltage-follower A₁ and A₂). The signals were subtracted with a differential amplifier (A₃), and recorded on the same screen of the CRO used to display the current pulse. The resistive component of the solution was analogically subtracted on the records. Thus the reported recordings and the *I/V* curves correspond to voltage deflections between the two faces of the bladder.

Voltage Scanning. Gallbladders were mounted in the chamber depicted in Fig. 1. This chamber was placed on the stage of a Leitz Laborlux Microscope (Wetzlar, West Germany) and was flat enough to permit observation of the epithelium. The preparation was visualized with a Zeiss (Oberkochen, West Germany) water immersion objective (40/0.75 W) with a long working distance which permits both a clear view of the intercellular spaces, and the positioning of the exploring microelectrode. The reference and exploring microelectrodes were made with aluminosilicate tubing with inner filament to quick filling (Federick Haer & Co., Brunswick) in a Brown-Flaming micropipette puller, Model P-77 (Sutter Instrument Co., San Francisco, Calif.) mounted on two Huxley micromanipulators. Microelectrodes were filled with 3 M KCl and, after beveling, had a resistance of 5–10 MΩ. The tip of the exploring microelectrode was located barely touching the desired spot on the apical border (noticeable by the spurious noise). In order to increase the accuracy of the location of the tip, the position of the microelectrode was always parallel to the junction. It formed with surface an angle of 25–30 degrees. A set of 1024 pulses of current were passed with a WPI 831 Pulse Generator, with an Interval Generator 830 and a Stimulus Isolator 830A (WP Instruments, Inc., New Haven, Conn.). The voltage deflections at the tip of the exploring microelectrode were differentially recorded with respect to a reference microelectrode located some 10 μm above, in a Nicolet digital averager (Instruments Corp. Madison, Wis.). The microelectrode was then raised 10 μm, a second set of 1024 pulses were passed, and again, the potentials were collected and subtracted from the first series. Signals were digitalized in the averager with 9 bit resolution, at 40 μsec per point and with a time constant of 0.1 to 1 msec. This procedure was adopted to improve the signal-to-noise ratio. As a control of the pulse protocol the pulses of injected current were also fed into the averager and subtracted, thus leading to no detectable signal. This insured that a voltage signal was not due to differences between the two sets of current pulses delivered. Short pulses with a positive and a negative deflection were sent to avoid ion accumulations. Each deflection lasted 5 msec and were separated by a 2-msec pause. Unless otherwise stated, their intensity was 32 μA cm⁻². The set-ups used to deliver and measure current and total membrane resistance were described previously (Cerejido et al., 1980).

In order to assess the spatial discrimination of the method when one maps in a horizontal plane, we placed a microelectrode in a petri dish with Ringer's solution and injected current through its tip. A second microelectrode was used to sense and measure the field thus produced at several distances on the side of the tip of the first (current-injecting) electrode. The size of the signals obtained dropped by 46 and 65% at 1 and 2 μm of the tip, respectively. If the mapping was done in a

horizontal plane 2 μm above the plane of the current-injecting microelectrode, the size of the signal collected was, of course, smaller. Nevertheless the spatial discrimination, as evaluated by the percentage decrease of the signal with sidewise displacements, remains the same. Thus, one may expect that, if microvillae, mucous, or other factors would not allow the exploring microelectrode to map at the exact horizontal plane of the apical border but, say, 1–2 μm above, the detection of conductive spots will not be impaired.

The bathing fluid contained (mM): 117.5 Na^+ , 2.5 K^+ , 1.8 Ca^{++} , 125.6 Cl^- , 2 imidazole⁺ and the pH was 7.4. Experiments were performed at room temperature.

Morphological studies

Gallbladders were cut open, washed as described, and the epithelium was fixed with 2.5% glutaraldehyde in 0.1 M sodium cacodylate buffer for 10 min. The epithelium was then detached by scraping with the edge of a glass coverslip

Transmission Electron Microscopy. After rinsing with buffer, samples were postfixed in 1% OsO_4 in sodium cacodylate buffer. Samples were blockstained with 1% aqueous uranyl acetate, dehydrated in a graded ethanol series, and embedded in Epon 812. Sections 0.5 μm thick, cut on glass knives, were stained with aqueous 1% toluidine blue. These sections were cut with diamond knives, picked up on Formvar-coated carbon-stabilized copper grids, stained with lead citrate and uranyl acetate and examined in a Zeiss EM10 electron microscope.

Scanning Electron Microscopy. Cell monolayers were fixed with glutaraldehyde and dehydrated. Critical-point drying from absolute ethanol into liquid CO_2 was carried out in a Technics (Springfield, U.S.A.) apparatus. Dried specimens affixed to aluminum stubs with double-sided tape were coated in an ion sputter JFC-1100 JEOL (Japan) evaporator with gold. Specimens were examined in a JEOL JSM 35C scanning electron microscope at 15 KV.

Freeze Fracture. Freeze-fracture replicas were obtained from epithelia fixed with 2.5% glutaraldehyde for 10 min as described above gradually infiltrated with glycerol up to 20% concentration, where they were left for 1 hr. They were then frozen in the liquid nitrogen. Freeze-fracture was carried out using a 300 Balzers apparatus equipped with a turbomolecular pump, at -120°C , and a vacuum of 2×10^{-6} mm Hg. After evaporation of platinum and carbon, replicas were recovered in sodium hypochloride, washed in distilled water, and mounted in Formvar-coated 100-mesh grids. Further details on the technique have been published elsewhere (Martinez-Palomo, Chávez & González-Robles, 1978). Observations were carried out with a Zeiss EM10 electron microscope. All micrographs of replicas are shown with the shadow direction from bottom to top.

Results are expressed as mean \pm standard error (number of observations).

Results

Current-Voltage Relation (I/V Curves)

Long transepithelial current flow in leaky epithelia is known to produce a marked time-dependent polarization effect (Frömter, 1972; Binslev et al., 1974). However, the instantaneous current-voltage

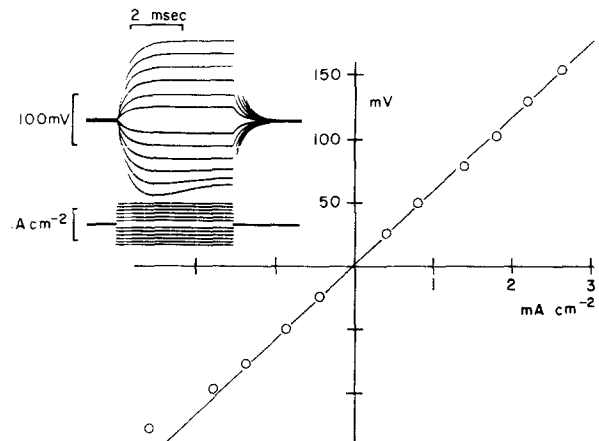


Fig. 2. Current-voltage relation of the *Necturus* gallbladder. The photograph shows paired records of voltage (above) and current pulses (below). In this and following Figures positive deflections refer to the positivity of the apical border. The I/V curve shown on the right of the Figure corresponds to the end of each pulse. The contribution of the bathing solution was analogically subtracted. Note that the curve remains linear at least from -1.6 (left) to $+2.6$ mA (right)

relation is linear (Wright, Barry & Diamond, 1971) which indicates that conductive pathways through the gallbladder are not altered by the passage of short-enough pulses. Therefore, the first step of this study was to select a duration and an intensity of current that will allow scanning with the microelectrode, without modifying the linearity of the I/V curve. Figure 2 shows the recording of the square current pulses of 5 msec (*below*) passed in both directions, and the corresponding voltage deflections (*above*). The I/V curve (*right*) was drawn with the amplitude at the end of each pulse. It may be seen that, with these short pulses, the I/V curve remains acceptably linear up to $+2.6$ and -1.6 mA cm^{-2} . For more negative currents there is a time-dependent increase in conductance. Accordingly, in the scanning studies described below we have used 2 pulses of 5 msec each, in both directions, separated by 2 msec and with an amplitude of $32 \mu\text{A cm}^{-2}$.

Characteristics of the Voltage Scanning

Figure 3 illustrates some characteristics of the procedure employed. The upper recording was made with a high current (not used in routine scanning) so as to increase the voltage deflection of a single voltage pulse. As explained in Materials and Methods, this voltage pulse (Fig. 3, second trace) was recorded between the exploring microelectrode and the reference electrode located 10 μm above. With the usual $32 \mu\text{A cm}^{-2}$ instead, deflection in this second pulse will not be observed, and a set of

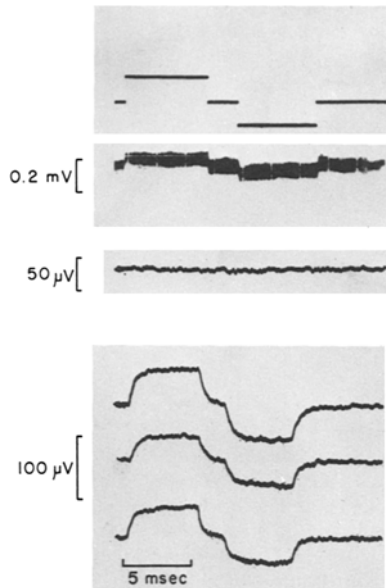


Fig. 3. This Figure intends to illustrate some characteristics of the procedure. *Above:* A large ($1600 \mu\text{A cm}^2$) current (upper trace) is passed to permit the illustration of a single (out of 1024) signal as recorded in the screen of the monitor oscilloscope (second trace). *Middle:* When the recording microelectrode is not raised, and both sets of 1024 pulses each are collected in the same spot, the subtraction gives a zero signal (third trace). This recording was made with the usual current of $32 \mu\text{A cm}^{-2}$. *Below:* The last three recordings were made on the same spot of an occluding junction to illustrate the reproducibility of the recordings

512 to 1024 is needed. The middle part of the Figure corresponds to two sets of 1024 pulses collected and subtracted without moving the microelectrode. It shows that the two sets cancel each other. Only if the second set is collected at a higher position (in this article $10 \mu\text{m}$), where the density of the current is lower, the subtraction leaves a clear signal. Finally, in the lower part of the Figure we recorded three times the same spot of an occluding junction to illustrate the reproducibility of the signal obtained.

If the epithelium were a perfectly flat surface, and the intercellular space a clean straight cut bathed by Ringer's solution, the lines of current will be concentrated in a vertical plane emerging from the junctions, and a microelectrode placed at a small (e.g. $1\text{--}2 \mu\text{m}$) lateral distance from the junction will detect a signal 40–70% smaller than at the maximum. However, Fig. 4 shows that a series of measurements made in a line that goes from the center of a cell body to the center of a neighbor through a line perpendicular to the junction, detects this junction even if the tip of the microelectrode is microns away. It also shows that the amplitude of the signal does not describe

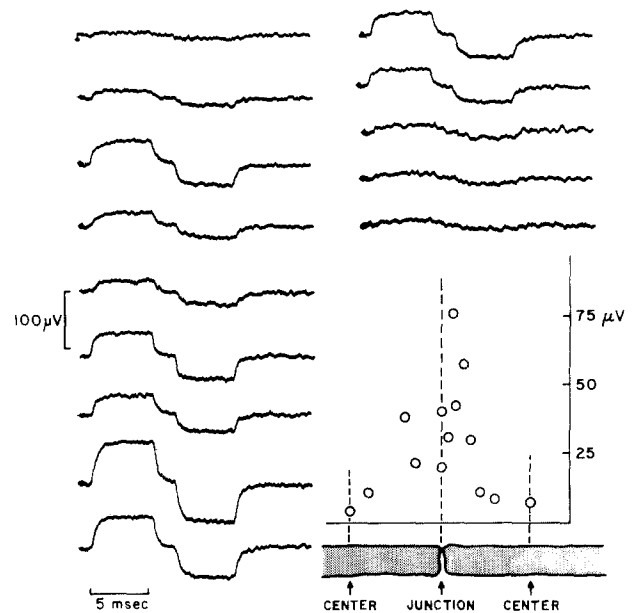


Fig. 4. Shape of the field near an occluding junction (schematized at the bottom right). Each signal was recorded in sequential order at a given spot in a line that crosses the junction perpendicularly. The graph represents the position (left to right) and the amplitude of the signals. The distance between the junction and a center is $12 \mu\text{m}$

a smooth bell, but recordings made at two very close positions may be considerably different. The shape of this bell resembles that of the field of an occluding junction in an MDCK monolayer. Further discussion of this point is postponed until we describe the morphological studies of the mouth of the interspace.

Figure 5 maps the conductance along the perimeter of a single cell as seen through the light microscope. The recordings show that (with the variation expected from the experiment in Fig. 4), the whole junction is conductive, and does not seem to alternate mute and active spots. This is different from the picture offered by the monolayer of MDCK cells mentioned in the Introduction. In this particular experiment the attention was concentrated on simple junctions, and intersections of the junctions of three neighbor cells were avoided, except for recording 5 taken for comparison. This is shown in Fig. 6, which summarizes the measurements made on junctions, center of cell bodies and intersections. It may be seen that, confirming Frömter and Diamond's observations, the intercellular spaces have a much higher conductance than cell bodies. In fact it is not certain whether the signals detected on the cell bodies correspond to current flowing through the cells, or belongs to the tailing off of the field at the junctions. It was expected that recordings on intersections between

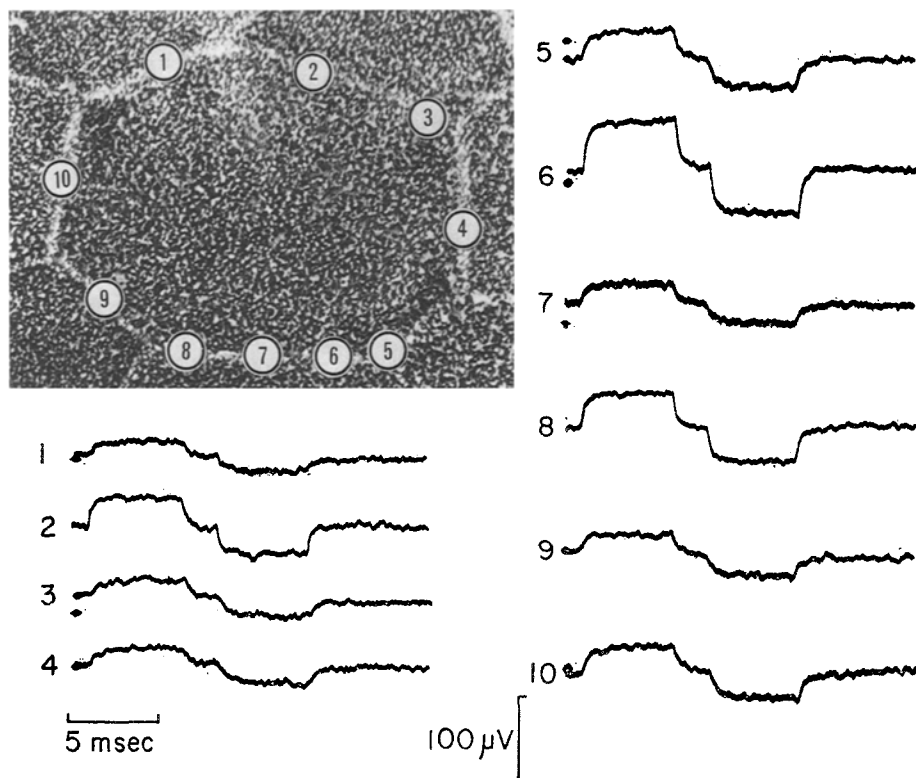


Fig. 5. Exploration of the perimeter of a single cell. Recordings were obtained at the points indicated on the cell. The picture of this cell was obtained by scanning electron microscopy and, of course, is not the one where the recordings were actually obtained. Yet the shape and size of the epithelial cells of the *Necturus* gallbladder are very similar and the composed Figure permits one to illustrate the experiment. Notice that signal 5 was recorded on a carrefour. The cell is 23 μm wide

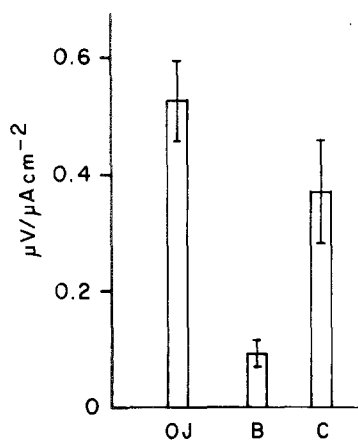


Fig. 6. Amplitude of the signals observed at junctions (OJ), center of cell bodies (B), and intersections (C). As explained in the text, the signals correspond to the difference in the electric field above a given spot of the monolayers and, therefore, should have the units of V cm^{-1} . Yet the sizes of the signals collected in the different experiments were normalized for the actual current used, which in a few experiments were not exactly $32 \mu\text{A cm}^{-2}$ but were between 20–35. The number of observations are 45, 24 and 17, respectively

three cells will afford greater signals, as the tip of the microelectrode will sense three (instead of two) half-junctions. Thus, the size of the signal on occluding junctions is $6.05 \pm 0.75 \mu\text{V}/\mu\text{A cm}^{-2}$ (Fig. 6) and, if intersections had 3/2 of this value,

their signals would have been $9.08 \pm 1.13 \mu\text{V}/\mu\text{A cm}^{-2}$. Since the value actually recorded at intersections was $4.2 \pm 1.0 \mu\text{V}/\mu\text{A cm}^{-2}$, i.e. much lower ($p < 0.005$), one may conclude that they have a lower conductance than the rest of the junctions around the cells. As shown below, this has a morphological counterpart.

Electron Microscopy

A thorough electron microscopic study of the *Necturus* gallbladder was performed by Bentzel et al. (1980). Our observations agree completely with their study and, therefore, our report concentrates on those aspects that bear directly on the localization of conductive pathways.

Scanning. The epithelium appears as a regular array of flat pentagonal or hexagonal cells homogeneously covered with microvillae. Two basic patterns of intercellular borders are observed: a protruding one where villi from each neighbor interdigitate (Fig. 7, left), and a second one where the cell contact gradually sinks below the level of the apical border (Fig. 7, right). The whole area is covered by surface coat that is retained in particular at the intercellular borders where, due to interdigitation, microvillae have a higher density (Fig. 8).

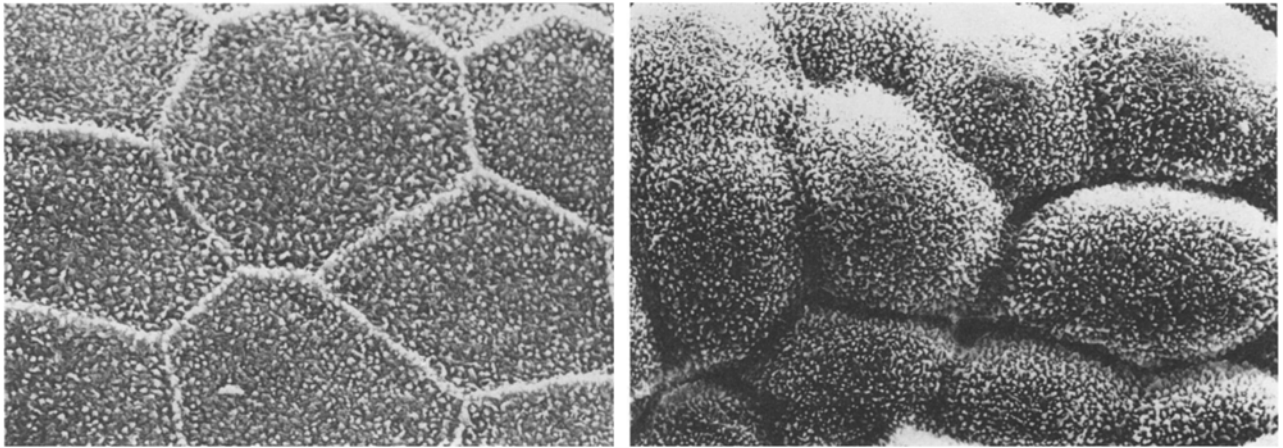


Fig. 7. Scanning electron microscopy. The dissected organ was cut open, washed with Ringer's solution, stretched with stainless steel pins, fixed and prepared as described in the text. In those areas where the epithelium was flat, the limits between neighbor cells (*left*) are clearly marked by a palisade of microvilli. In other areas (*right*), in particular at the concavity of wrinkle creases, the apical portion of the cells protrudes, thus hiding the mouth of the intercellular space. (2,190 ×)

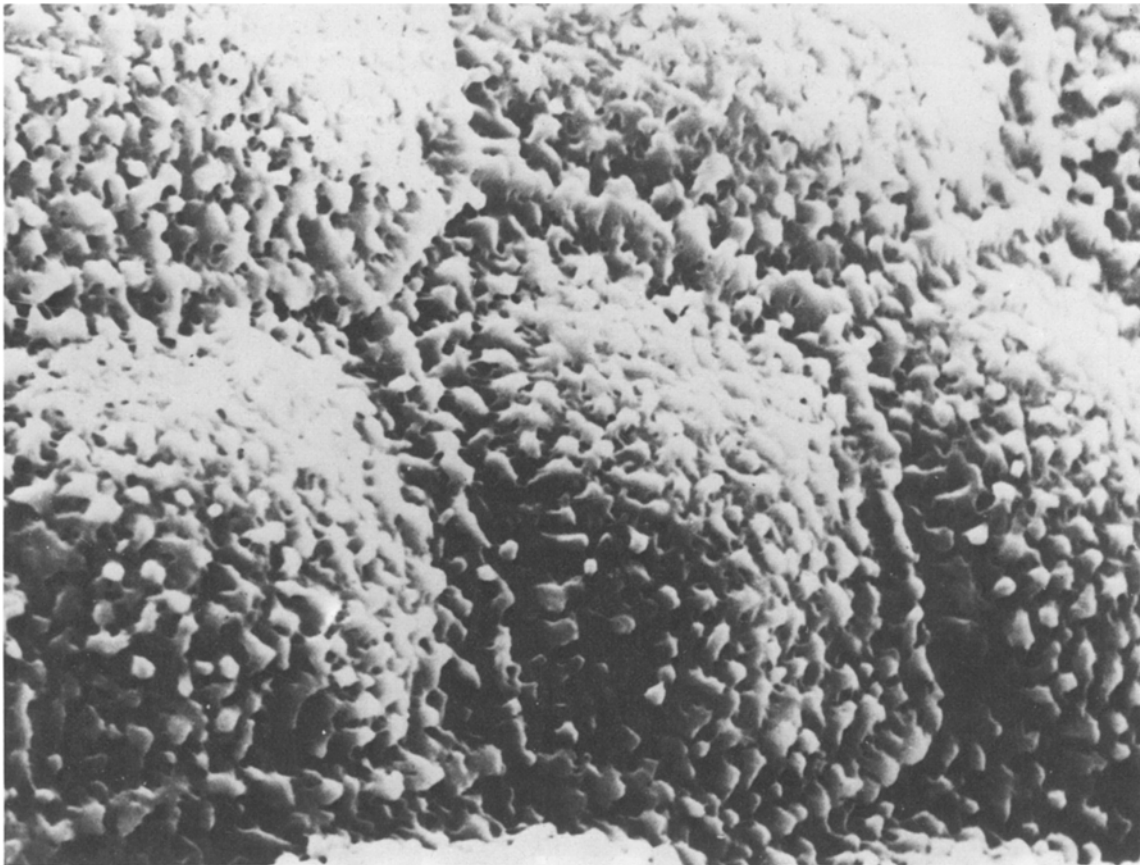


Fig. 8. Scanning electron micrograph taken from a slant angle showing the crest formed by the microvilli of the neighboring cells. Note the surface coat covering the microvilli

Transmission Electron Microscopy. Two morphological characteristics seem to be worth emphasizing for the present study. The first one concerns the mouth of the interspace which is not a sharp perpendicular cut, but opens gradually and, in

many cases, obliquely to the apical border (Fig. 9). It is also covered by microvilli from both cells in a manner that one would expect to spread and scatter any stream of fluid or current coming from the interspace. The second morphological charac-

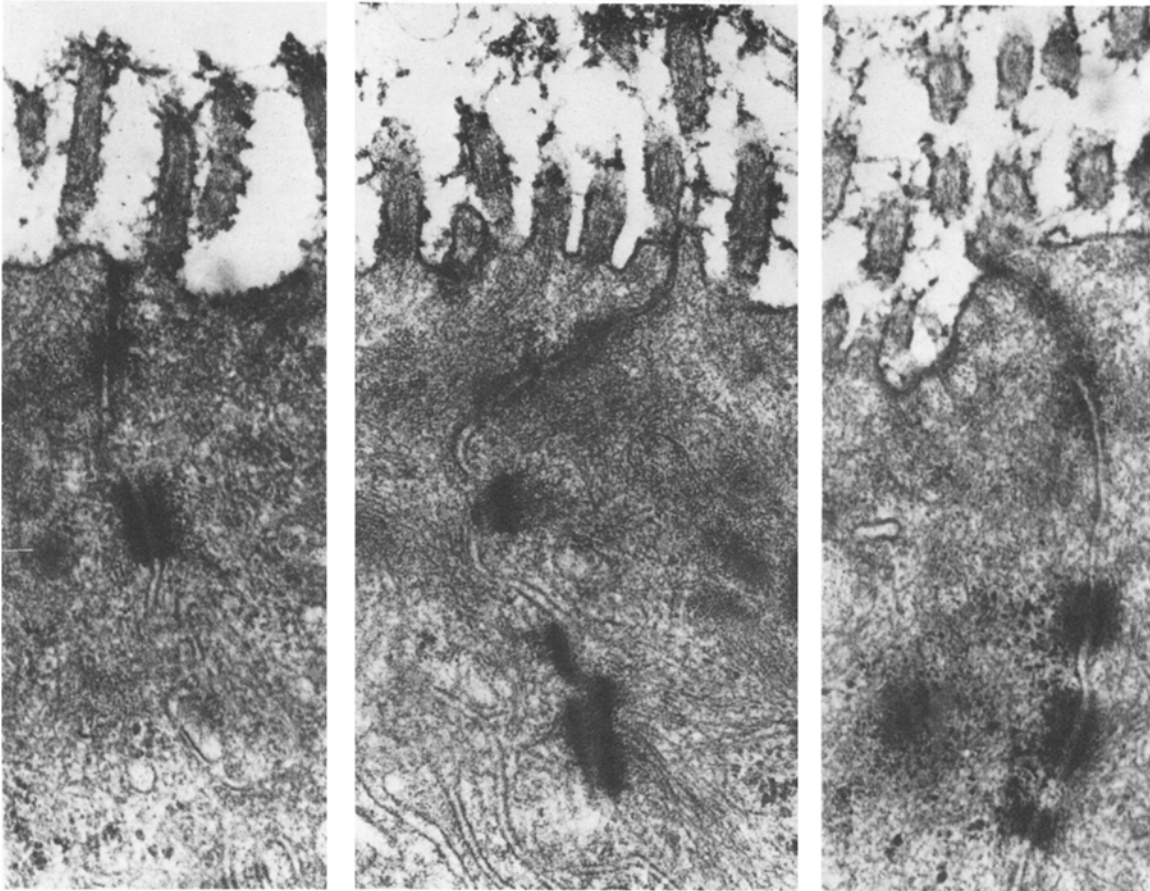


Fig. 9. Thin-section electron microscopy of a gallbladder showing the apical end of three intercellular spaces. The apical border has a dense population of microvilli. The intercellular space on the left is straight and reaches the apical border perpendicularly. The one on the center deviates toward the right. The influence that this nonperpendicular exit might have in the interpretation of the electrical measurement is discussed in the text. The junction on the right bends and finally opens almost horizontally. In all cases the apical region of the intercellular space is profusely covered by microvilli. (3,000 \times)

teristics which may influence the interpretation of the present results is illustrated in Fig. 9 (center): the interspace approaches the apical border in a somewhat perpendicular direction but, just before reaching this border, it bends to one side and emerges on the top of the neighbor cell. It is conceivable that under the light microscope used in the voltage-scanning procedure, one would see the interspace at one point (and place the microelectrode there) while the stream of current flows approximately one micron away where the opening is.

Freeze Fracture. The occluding junctions of the *Necturus* gallbladder appear as a belt-like network of ridges on *P* faces and complementary furrows on *E* faces (Fig. 10). Claude and Goodenough (1973) and Claude (1978) have postulated that the electrical resistance across the epithelium is pro-

portional to the number of strands. The regular number of strands and homogeneous width of the junctional belt (Fig. 10) in *Necturus* gallbladder epithelial cells are evident. Figure 10 shows another morphological feature which is likely to bear on the interpretation of electrical results: at the intersections between three cells the width of the junction increases markedly. This structure was first described by Staehelin, Mukherjee and Williams (1969) in the rat intestine and confirmed by Friend and Gilula (1972). If the electrical resistance of the occluding junction is actually proportional to the number of strands, intersections would have a lower conductance than the rest of the occluding junction. However, according to a detailed analysis made by Staehelin (1973), the arrangement of the sealing element of the three adjoining cells may form a central "tube", which would presumably increase the permeability of the intersection.

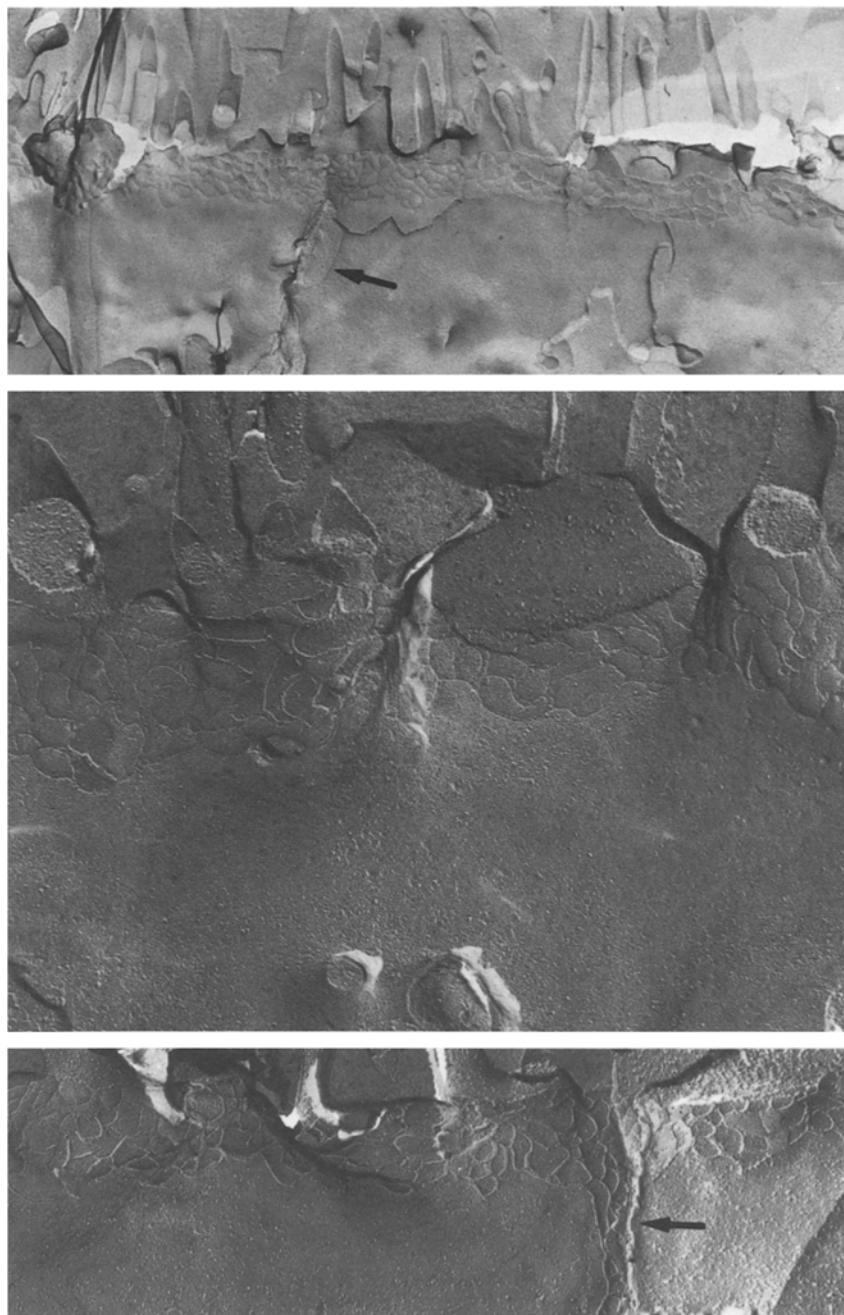


Fig. 10. Above. Replica of freeze-fractured *Necturus* gallbladder showing that the occluding junction occupies a belt constituted of membrane strands. The number of strands (4 to 7), in the apico/basal direction is relatively uniform (40,000 \times). This is shown in detail in the central and lower pictures (70,000 \times). Note that at the arrows, which correspond to an intersection between three neighbor cells (carrefour), the junction expands abruptly toward the basal region

Miscellaneous Observations. In the course of the studies reported above we made some circumstantial observations which were not systematically investigated. Among them: (1) *Effect of mechanical pressure* (Fig. 11). The microelectrode is used in a position parallel and superimposed to the image of the junction. If it is lowered, so as to press the occluding junction, the amplitude of the signals increases. This effect is immediately reversible: it disappears as soon as one makes a second set of recordings on the same spot without pressing, and

reappears when one presses again. However, we could not elicit the pressure effect in all the junctions. While the reason for this failure is not obvious, one of the simplest interpretations for the effect of pressure is that, if favorably oriented, i.e. if the lips are not overlapping, pressure detaches the junction under the microelectrode. (2) *Cellular damage?* The low electrical resistance of leaky epithelia was initially associated to cellular damage, death and desquamations (Clarkson, 1967). In the course of two experiments we found small groups

(3–4 cells) of swollen and granular cells that were assumed to be damaged. Figure 12 shows that recordings on the center of one of these cells afforded ample signals, some 4–5 times higher than those recorded on a regular-looking cell located some 10 cells apart. These recordings were made using a very high current ($1600 \mu\text{A cm}^{-2}$) to enhance the small signals usually obtained on cell bodies. We cannot distinguish whether these atypical cells were originally present in the gallbladder or were produced during the handling of the preparation, but their occurrence in a given bladder is very rare, and was observed in only two (out of 12) bladders scanned.

Discussion

The studies by Frömter and Diamond (1972) quoted in the Introduction led to two main conclusions: (1) the high conductance of leaky epithelia does not depend on a transcellular route; and (2) it is located at the intercellular space limited by an occluding junction. The present study using shorter (5 *vs.* 1200 msec) and smaller pulses (32 *vs.* $2000 \mu\text{A cm}^{-2}$) confirms these conclusions. On the basis of the present data we may add: (1) the conductance measured over the apical surface of the epithelium is evenly distributed around the perimeter of the cells all over the length of occluding junctions, except at intersections between three cells; (2) the conductance at these intersections is not higher than at junctions; and (3) the width of the junction, as well as the number of junctional strands as seen in freeze-fracture replicas, is evenly distributed until one reaches an intersection where the junction expands toward the basal region. Therefore we shall elaborate on these points.

If the intercellular space were a perpendicular cut describing a straight line in the plane of a naked flat epithelium, the main variables in the shape of the field produced by the current pulses would be: (a) the conductance of the Ringer's, that would tend to "verticalize" the lines of current, and (b) the surface conductance of the cell membranes, that would tend to carry the current sidewise. However, the real intercellular space: (a) follows a tortuous line on the epithelium (Fig. 7), (b) is not perpendicular (Fig. 9), (c) is covered with surface coat; (d) microvilli interdigitate over the interspace (observations made with a high voltage electron microscope which will be published separately), thus producing electrically blind spots, and (e) even the apical surface is not a perfectly horizontal plane. Nevertheless, the shape of the bell above a given junction, although irregular, has an ampli-

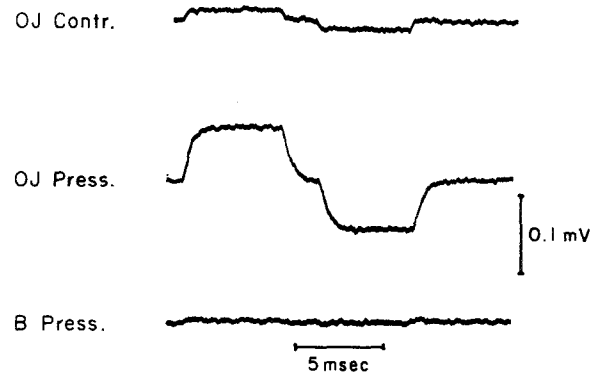


Fig. 11. Effect of mechanical pressure. In some areas, when the signals were recorded with the microelectrode pressing the intercellular space, the amplitude of the signal was enhanced (*OJ Contr.*: occluding junction, control; *OJ Press.*: occluding junction, pressing). This effect cannot be elicited on the body of the same cell (*B: Press.*: cell body, pressing)

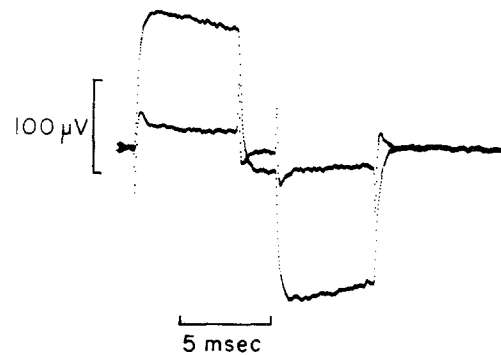


Fig. 12. Cellular damage? The trace with higher amplitude was recorded on the center of a cell whose aspect (brown, swollen, granular) suggested that it was damaged. The electrical resistance of this particular bladder was $250 \Omega\text{cm}^2$. The smaller signal was recorded with the same high current ($1600 \mu\text{A cm}^{-2}$) some 10 cells away from the reputedly damaged cell

tude and width similar to the one produced by the tip of a current-injecting microelectrode placed at the bottom of the chamber (*see* Materials and Methods). Also, the size of the signal decreases some 80% when the electrode is placed half way from the border to the center of the cell (Fig. 4) and, at this center, signals reduce to 17% from the value at the junction (Fig. 6: $B/OJ=0.17$). These considerations allow two conclusions: (1) that a given conducting spot would not escape detection because of critical positioning of the microelectrode, and (2) that the irregularities in the electric field introduced by the factors listed above, do not permit quantitative comparisons between two neighbor points along the junctions. Furthermore, since the spatial discrimination of the method is in the order of microns, one cannot discriminate whether the intercellular space is a long, continuous slit, or else is a perfectly sealed region con-

taining a row of discrete pores with radii in the order of angstroms.

Although the resistance of occluding junctions have been assumed to be proportional to the number of strands (Claude & Goodenough, 1973; Pricam, Humbert, Perrelet & Orci, 1974; Kühn and Reale, 1975) and a hypothesis was advanced to account for such correlation (Claude, 1978) the number of strands may not be the only factor. Thus Martínez-Palomo and Erij (1975) have shown that the rabbit intestinal mucosa and the frog urinary bladder, with a similar number of junctional strands, have an electrical resistance two orders of magnitude apart. The lateral intercellular space also seems to play an important role (Smulders, Tormey & Wright, 1972; Wright, Smulders & Tormey, 1972; Wiedner & Wright, 1975). Another clear indication that the number of strands is not the only factor controlling junctional resistance is that gallbladder resistance varies considerably as one varies pH (Wright & Diamond, 1968; Moreno & Diamond, 1974; Reuss, Cheung & Grady, 1981). The information available at present tends to indicate that, while in a given organ (e.g. a kidney) the number of strands in different portions may bear a close relation with the electrical resistance, this relation does not hold when comparing two epithelia in different organs, or even in different animal species. In the particular case of the *Necturus* gallbladder, Bentzel et al. (1980) have demonstrated that the occluding junction undergoes rapid and reversible rearrangements of the strands with concomitant changes in the transepithelial permeability. The fact that intersections, where three junctions contribute, do not have a higher conductance, and that this is associated with a wider and more populated junction, is in keeping with the observations of these authors. It may not be assumed though, that at intersections the junction has, simply, more strands. Detailed studies of this region performed by Staehelin et al. (1969), Friend and Gilula (1972) and Staehelin (1973) have shown that the sealing elements form a central "tube". The electrical studies reported in this article would not support the existence of a high conductive element in this region which would be opened under the experimental conditions we used.

As mentioned in the Introduction, we have cultured monolayers of MDCK cells on permeable supports (a disk of Nylon cloth coated with collagen) and performed voltage-scanning studies on their occluding junctions (Martínez-Palomo, Meza, Beaty & Cerejido, 1980; Meza, Ibarra, Sabanero, Martínez-Palomo & Cerejido, 1980; Cer-

eijido, Meza & Martínez-Palomo, 1981). The mouth of these junctions have characteristics similar to the *Necturus* gallbladder, except that the population of villi is far more sparse. While in the present study of the *Necturus* gallbladder we have observed that all junctions are conductive, in the monolayer of MDCK cells we found long segments of intercellular space without detectable signals. On the basis of the shape of the field on conductive spots (Fig. 4 of the present paper, and Fig. 8 of the paper on MDCK [Cerejido et al. 1980]) one may conclude that these areas are not due to lack of detection, but may represent junctions that are actually *tight*.

Our observations on *Necturus* gallbladder and on MDCK monolayers indicate that, while the junctions of the MDCK monolayers are essentially tight, but studded with conductive spots, the ones on the *Necturus* gallbladder may be visualized as homogeneous conductors, which are slightly more tight at the intersections. Finally one may emphasize that by saying *homogeneous conductor*, we do not discard the possibility that the occluding junctions of the *Necturus* were sealed regions containing pores of the size of univalent ions.

We wish to acknowledge the economical support of the Consejo Nacional de Ciencia y Tecnología de México, and the Public Health Service of the United States AM 26481-PHY.

References

- Bentzel, C.J., Hainau, B., Ho, S., Hui, S.W., Edelman, A., Anagnostopoulos, T., Benedetti, E.L. 1980. Cytoplasmic regulation of tight-junctions permeability: Effect of plant cytokinins. *Am. J. Physiol.* **239**:C75-C89
- Bindslev, N., Tormey, J. McD., Wright, E.M. 1974. The effects of electrical and osmotic gradients on lateral intercellular spaces and membrane conductance in a low resistance epithelium. *J. Membrane. Biol.* **19**:357-380
- Cerejido, M., Meza, I., Martínez-Palomo, A. 1981. Occluding junctions in cultured epithelial monolayers. *Am. J. Physiol.* **240**:C96-C102
- Cerejido, M., Robbins, E.S., Dolan, W.J., Rotunno, C.A., Sabatini, D.D. 1978. Polarized monolayers formed by epithelial cells on a permeable and translucent support. *J. Cell Biol.* **77**:853-880
- Cerejido, M., Stefani, E., Martínez-Palomo, A. 1980. Occluding junctions in a cultured transporting epithelium: Structural and functional heterogeneity. *J. Membrane Biol.* **53**:19-32
- Clarkson, T.W. 1967. The transport of salt and water across isolated rat ileum. Evidence for at least two distinct pathways. *J. Gen. Physiol.* **50**:695-727
- Claude, P. 1978. Morphological factors influencing transepithelial permeability: A model for the resistance of the zonula occludens. *J. Membrane Biol.* **39**:219-232
- Claude, P., Goodenough, D.A. 1973. Fracture faces of zonulae occludentes from "tight" and "leaky" epithelia. *J. Cell Biol.* **58**:390-400

- Friend, D.S., Gilula, N.B. 1972. Variations in tight and gap junctions in mammalian tissues. *J. Cell Biol.* **53**:758-776
- Frömter, E. 1972. The route of passive ion movement through the epithelium of *Necturus* gallbladder. *J. Membrane Biol.* **8**:259-301
- Frömter, E., Diamond, J. 1972. Route of passive ion permeation in epithelia. *Nature, New Biol.* **235**:9-14
- Kühn, K., Reale, E. 1975. Junctional complexes of the tubular cells in the human kidney as revealed with freeze-fracture. *Cell Tissue Res.* **160**:193-205
- Martínez-Palomo, A., Chávez, B., González-Robles, A. 1978. The freeze-fracture technique: Applications to the study of animal plasma membranes. In: Electron Microscopy, Vol. 3. State of the Art Symposia. J.M. Sturgess (editor). pp. 503-515 Micros. Society of Canada, Toronto
- Martínez-Palomo, A., Erij, D. 1975. Structure of tight junctions in epithelia with different permeability. *Proc. Natl. Acad. Sci. USA* **72**:4487-4491
- Martínez-Palomo, A., Meza, I., Beaty, G., Cerejido, M. 1980. Experimental modulation of occluding junctions in a cultured transport epithelium. *J. Cell Biol.* **87**:736-745
- Meza, I., Ibarra, G., Sabanero, M., Martínez-Palomo, A., Cerejido, M. 1980. Occluding junctions and cytoskeletal components in a cultured transporting epithelium. *J. Cell. Biol.* **87**:746-754
- Misfeldt, D.S., Hamamoto, S.T., Pitelka, D.K. 1976. Transepithelial transport in cell culture. *Proc. Natl. Acad. Sci. USA* **73**:1212-1216
- Moreno, J.H., Diamond, J.M. 1974. Discrimination of monovalent inorganic cations by "tight" junctions of gallbladder epithelium. *J. Membrane Biol.* **15**:277-318
- Pricam, C., Humbert, F., Perrelet, A., Orci, L. 1974. A freeze-etch study of the tight junctions of the rat kidney tubules. *Lab. Invest.* **30**:286-291
- Reuss, L. 1978. Transport in gallbladder. In: Membrane Transport in Biology. G. Giebisch, D.C. Tosteson, and H.H. Ussing, editors. Ch. 17, Pt. IV. A and B Transport Organs. Springer-Verlag, Berlin, Heidelberg, New York
- Reuss, L., Cheung, L.Y., Grady, T.P. 1981. Mechanism of cation permeation across apical cell membrane of *Necturus* gallbladder: Effects of luminal pH and divalent cations on K^+ and Na^+ permeability. *J. Membrane Biol.* **59**:211-224
- Reuss, L., Finn, A.L. 1977. Effects of luminal hyperosmolarity on electrical pathways of *Necturus* gallbladder. *Am. J. Physiol.* **232**:C99-C108
- Smulders, A.P., Tormey, J. McD., Wright, E.M. 1972. The effect of osmotically induced water flows on the permeability and ultrastructure of the rabbit gallbladder. *J. Membrane Biol.* **7**:164-197
- Staehein, L.A. 1973. Further observations on the fine structure of freeze-cleaved tight junctions. *J. Cell Sci.* **13**:763-786
- Staehein, L.A., Mukherjee, T.M., Williams, A.W. 1969. Freeze-etch appearance of tight junctions in the epithelium of small and large intestine of mice. *Protoplasma* **67**:165-184
- Wiedner, G., Wright, E.M. 1975. The role of the lateral intercellular spaces in the control of ion permeation across the rabbit gallbladder. *Pfluegers Arch.* **358**:27-40
- Wright, E.M., Barry, P.H., Diamond, J. 1971. The mechanism of cation permeation in rabbit gallbladder. *J. Membrane Biol.* **4**:331-357
- Wright, E.M., Diamond, J.M. 1968. Effect of pH and polyvalent cations on the selective permeability of gallbladder epithelium to monovalent ions. *Biochim. Biophys. Acta* **163**:57-74
- Wright, E.M., Smulders, A.P., Tormey, J. McD. 1972. The role of the lateral intercellular spaces and solute polarization effects in the passive flow of water across the rabbit gallbladder. *J. Membrane Biol.* **7**:198-219

Received 8 December 1981; revised 30 April 1982